

Research Article

Direct Deposition of Micron-Thick Aligned Ceramic TiO₂ Nanofibrous Film on FTOs by Double-Needle Electrospinning Using Air-Turbulence Shielded Disc Collector

T. Krishnamoorthy,^{1,2} V. Thavasi,² V. Akshara,³ A. Senthil Kumar,⁴ D. Pliszka,²
S. G. Mhaisalkar,¹ and S. Ramakrishna^{2,4,5}

¹ School of Materials Science and Engineering, Nanyang Technological University, 50 Nanyang Avenue, Singapore 639798

² NUS Nanoscience and Nanotechnology Initiative (NUSNNI), Faculty of Engineering,
National University of Singapore, Singapore 117576

³ Amity Institute of Nanotechnology, Amity University, Sector-125, Noida 201301, India

⁴ Department of Mechanical Engineering, National University of Singapore, Engineering Drive 3, Singapore 117576

⁵ King Saud University, Riyadh 11451, Saudi Arabia

Correspondence should be addressed to V. Thavasi, velnanotech@gmail.com

Received 30 June 2011; Accepted 22 August 2011

Academic Editor: Renzhi Ma

Copyright © 2011 T. Krishnamoorthy et al. This is an open access article distributed under the Creative Commons Attribution License, which permits unrestricted use, distribution, and reproduction in any medium, provided the original work is properly cited.

One-dimensional (1D) metal oxides, typically nanowires and nanorods, have unique electronic and optical properties due to quantum phenomena that find applications in modern energy and electronic devices. We present here the electrospinning method that produces the aligned TiO₂ nanofibres directly on the fluorine-doped tin oxide (FTO) substrates mounted rotating disc collector. The aligned TiO₂ ceramic nanofibres mat of 6 μm thickness is achieved in 4 h using a nonconductive enclosed-air-shield with air-hood design over the FTO mounted rotating disc collector. The aligned TiO₂ nanofibers are found to retain its integrity and binding on FTO surface even after sintering at 500°C. SIMON 8 modeling package is used to determine the behaviour of the charged polymer/TiO₂ jet when single and double needles are used for electrospinning process. The simulation study reveals that the repulsive force of the charged fibers from the double needle exerts stronger electric field distribution along the flow of stream that results in the reduction of the fibers diameter, which is about 28 nm than that of using single-needle system.

1. Introduction

Metal oxide semiconductors exhibit unique electronic and optical properties in its one-dimensional (1D) morphology as the self-organization of charges occurs in 1D form via interaction energy minimization. A highly ordered 1D nanostructure is preferred to enhance the performance of electronic and photonic devices. It has been reported that the ordered 1D nanostructure enabled for larger current generation by improving the charge separation and electron transport in polymers and oxides [1–4]. For example, the ordered nanostructure has improved the gas sensing property of ZnO compared to that of random structure [5]. Likewise, the orderly aligned SnO₂ nanoboxes have improved the electron transport [6]. Numerous methods such as electric

field directed assembly, flow-assisted alignment, selective chemical patterning, laser, photolithography [7], self-assembly [8–10], and Langmuir-Blodgett (LB) technique [11] have been explored to align the metal oxides and polymers.

Electrospinning is another competent technique that has also been employed to produce 1D polymers and metal oxides [12–16]. The simple electrospinning often produces intertangled nanofibres after deposition which could cause the insufficient exposure of the faces and edges of fibres. Furthermore, a film made by simple electrospinning contains random arrangement of fibres, with different length, which might impose poor reproducibility when prepared as electroactive layer. Alignment of materials as nanofibres creates greater compactness, and the aligned architecture could accommodate more quantity of material per unit area that

support for the miniaturisation of the electronic devices. The aligned nanofibres were successfully produced by researchers in electrospinning using the rotating disc as collector and at higher speed. However, available electrospinning methods are limited by their capability to produce aligned metal oxide nanofibers of higher thickness. For instance, the nano TiO_2 film should possess the thickness of 0.5–2.0 μm and 8–30 μm for solid state and liquid state dye sensitized solar cells (DSSC), respectively, because such thick film supports for significant electron diffusion [17–20]. In literatures, the maximum thickness of the aligned nanofibres obtained using electrospinning so far was only about 250 nm [21]. Hence, there is a great demand for the production of aligned metal oxide nanofibers with the higher thickness, in shorter time, and with good reproducibility. Aligning the nanofibers directly on the conductive fluorine-doped tin oxide (FTO) substrate for various applications such as optoelectronic and photovoltaics are preferred as such technique shortens two conventional steps in electrospinning: preparation of well-ordered fibres and the deposition of these fibres on FTO using doctor blade/or dip casting. However, currently available techniques impose major challenge due to complexity in the steps that convert the composite fibers into ceramic fibers. Sintering at 400–550°C, an important process that converts TiO_2 /polymer nanofibres into ceramic structure by bridging between the grains, is believed to enhance electron/charge carrier mobility in the film. The stress is developed on the nanofibers during sintering, and when exceeding the internal resistance of the nanofibers, the peeling-off FTO occurs. Therefore, in addition to the better alignment, the bondage of ceramic nanofibers onto the conductive substrate is critical for device applications.

In this work, the TiO_2 nanofibres have been produced and aligned directly on FTO using the modified electrospinning setup. A nonconductive air-shield has been introduced in electrospinning setup that facilitated for the production of micron thick ceramic TiO_2 nanofibres film. The method developed in this study can be extended to control the alignment and thickness in large scale for metal-oxide-based solar cells and sensors.

2. Experimental

The precursor for TiO_2 was prepared by dissolving 0.2 g of polyvinylpyrrolidone (PVP, MW of 1.6×10^6 g/mol) and 0.5 g of titanium tetra-isopropoxide (Aldrich) in 3.5 mL of ethanol (AR grade). 1 mL of acetic acid was added into the solution. The solution was then loaded into a plastic syringe equipped with a 27 1/2 gauge needle (Becton Dickson). The diameter of the rotating disc was 20 cm. To obtain more samples, six FTOs (1 mm-thick, Asahi Glass) with a sheet resistance of 15 Ω were mounted over the six plastic holders affixed using scotch tape on the edge of the disc at equal space (Figure 1). A small 1×1 cm² of aluminium foil was attached such that it wrapped both the back of the holders and the top side of FTO. The conductive wire was hooked to the foil using double-side tape, which made FTO grounded. This allowed the nanofibres to be collected directly onto

TABLE 1: Effect of design modification in electrospinning.

Electrospinning	Design modification	Collection time (h)	Thickness of sintered aligned TiO_2 nanofibres (μm)
Single needle	Without shield	4	0.5
	Top-air-shield	4	1.5
	Enclosed-air-shield	4	4
	Enclosed-air-shield and air-hood	4	4
Double needle	Enclosed-air-shield and air-hood	4	6

the FTOs. The syringe pump flow rate of 0.2 mL/h was set up. A distance of 10 cm between the needle tip and the edge of rotating disc was set up, and the potential of 15 kV was applied between them. The speed of the rotating disc was held constant at 750 rpm for all the experiments. All the electrospinning experiments were performed at room temperature. A nonconductive block of size 24 cm \times 24 cm was designed and introduced as top-air-shield over the rotating disc collector (Figure 1(b)) and compared the effect of alignment and thickness of film obtained using the setup without any shield. For another study, an enclosed-air-shield (24 cm \times 24 cm) with the slit dimension of 22 cm \times 3.5 cm was fabricated and positioned as shown in Figure 1(c). For the third set of experiment, an air-hood of size (14 cm \times 3.5 cm) was affixed just behind the slit of the enclosed shield (Figures 1(d) and 1(e)).

3. Results and Discussion

Better the alignment of fibers is, the larger will be the quantity of materials per unit area as illustrated in Figure 2, which are beneficial for device applications. For example, dye adsorption on the nanosized TiO_2 is the critical factor in improving the performance because anchored dye molecules absorb more photons thus results in larger photocurrent. The aligned nanofibres architecture could improve the photon conversion efficiency and charge separation.

Figure 3(a) shows the SEM images of TiO_2 nanofibres obtained when rotating the disc at 750 rpm, but without air-shield. The average diameter of the green nanofibres (TiO_2 /PVP) was found to be 180 ± 20 nm. The collected nanofibres on each FTO substrate were first hot pressed at 120°C and for 15 min as a pretreatment to sintering. Then the samples were introduced for sintering in the tubular furnace at 500°C for 3 h with the ramp rate of 1°C/min and cooled down to 30°C with the rate of 1°C/min. The sintered TiO_2 nanofibres were observed to possess the diameter of 98 ± 20 nm. All the film thicknesses reported in this work are the measurement of the ceramic TiO_2 nanofibers after sintering (Table 1).

During electrospinning without air shield, it was observed that the majority of the TiO_2 /PVP nanofibres were

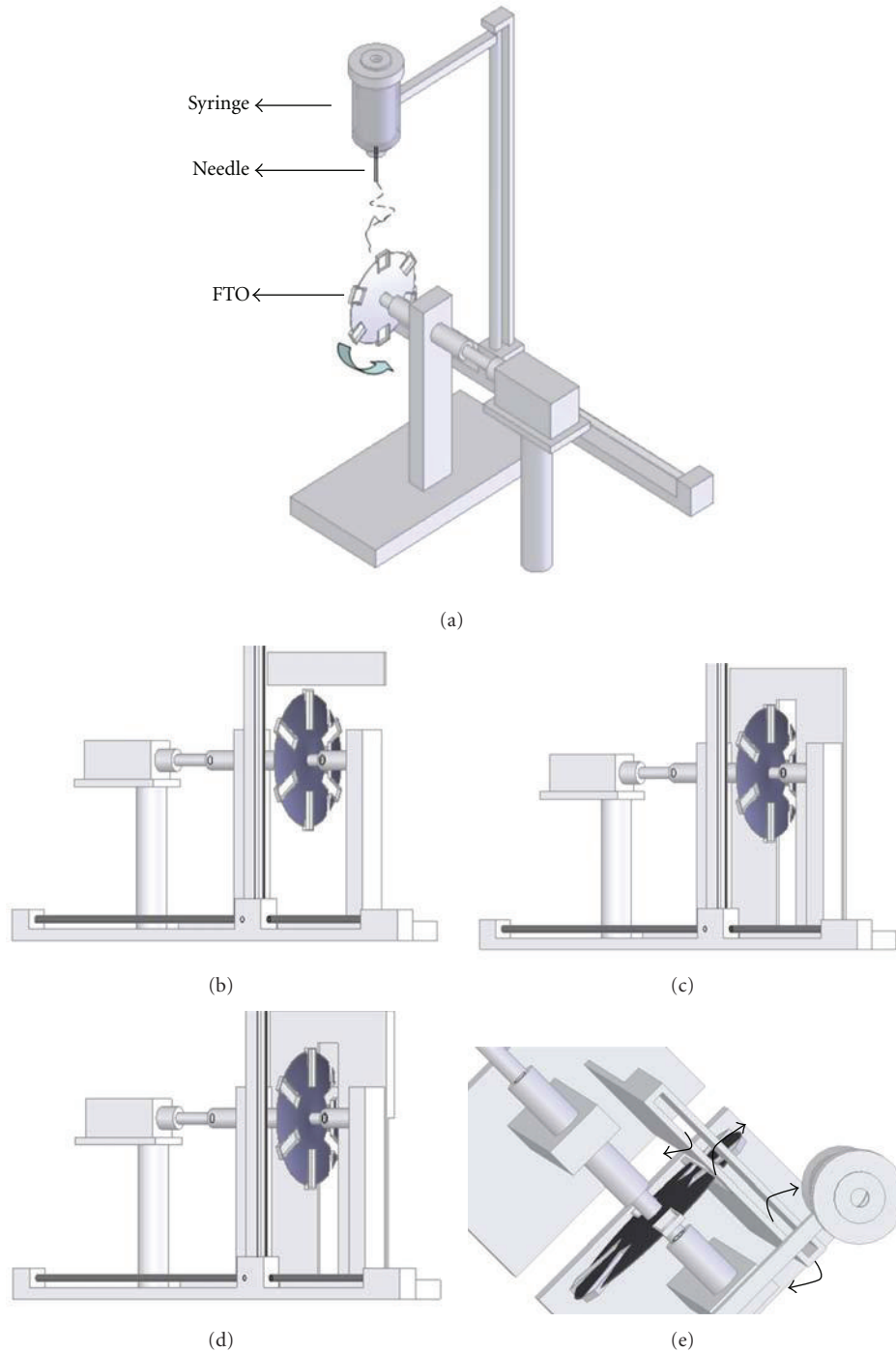


FIGURE 1: (a) Experimental setup of electrospinning. The metal oxide precursor is taken in a syringe. 1-mm-thick six FTOs are fixed on the holder mounted on rotating disc at equal space. The rotating disc of diameter 20 cm with (b) top-shield, (c) enclosed-air-shield, (d) enclosed-air-shield with air-hood (front view), and (e) air-hood arrangement (top view) for the turbulent air to escape.

flown away from the deposition area (FTO). This was due to the velocity of the rotating disk. Rotation at 750 rpm guided for better alignment of nanofibres; however, the disk at such speed generates the turbulent wind inward direction that carries the nanofibres away from the deposition area as the fibres were nano in size, which results in more wastage of

TiO₂, and also affects its alignment. This yielded the poor thickness of the collected aligned nanofibres for 4 h, which was about 500 nm.

The nanofibres shown in Figure 3(b) were collected at 750 rpm with top-air shield. With top-air-shield arrangement, the rate of nanofibres deposition was improved to

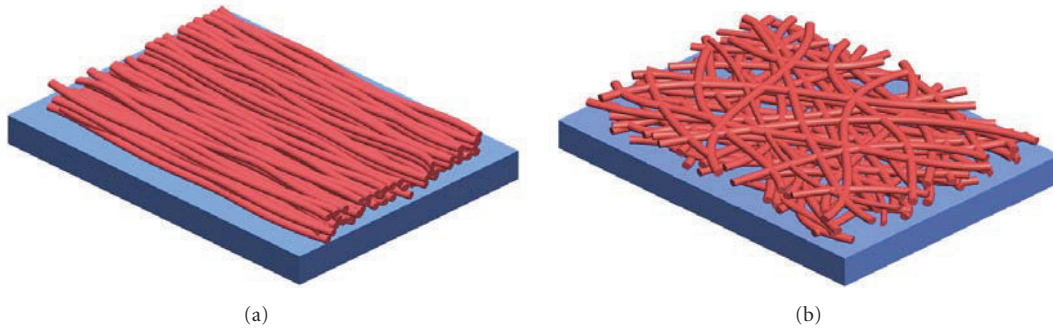


FIGURE 2: Schematic of (a) aligned TiO_2 nanofibres and (b) random TiO_2 fibres.

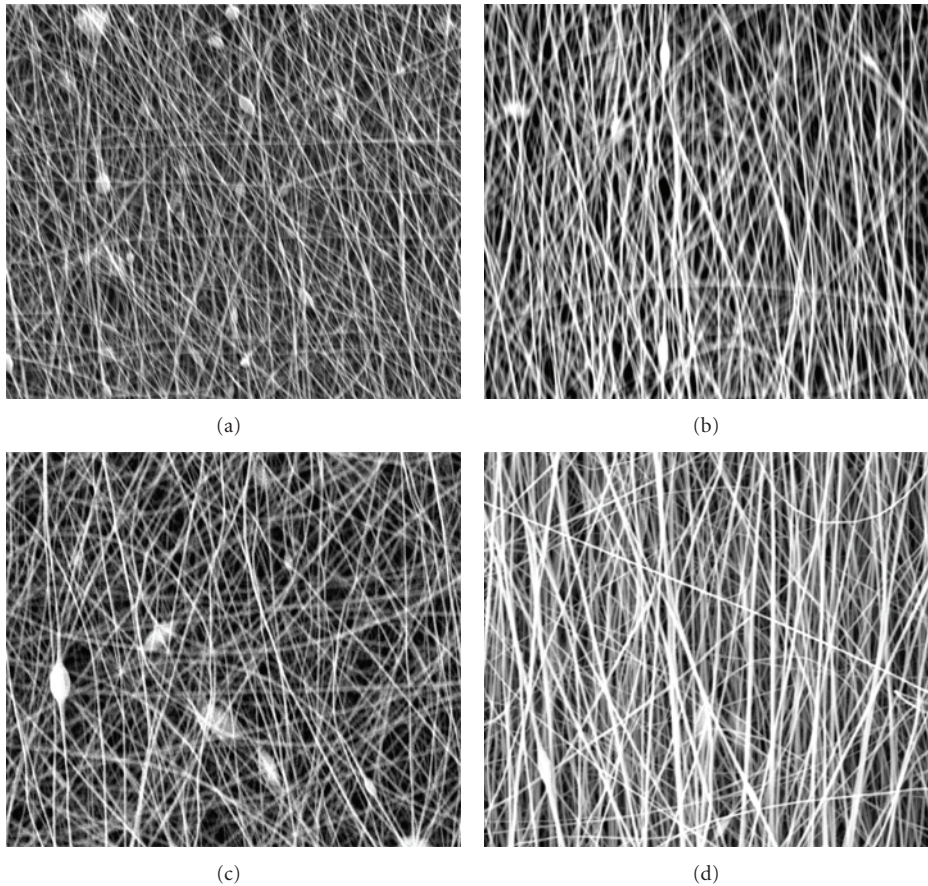


FIGURE 3: The TiO_2 ceramic nanofibres of diameter 98 ± 20 nm were collected using the rotating disc at 750 rpm; (a) without air shield, (b) using top-air shield, (c) using enclosed-air-shield, (d) using enclosed-air-shield with air-hood.

$1.5 \mu\text{m}$ in 4 h compared to the electrospinning without any shield. The alignment was substantially improved by the insertion of the top-air shield, and the nanofibres were nearly bead-free. The top-air-shield reduced the wind generated by the rotating disc, in turn enabled to align the nanofibres over the FTOs. The nanofibres alignment was found to be decreased gradually after hours of electrospinning. The poorer alignment was observed mainly due to the turbulence wind from the disc that disturbs the nanofibres deposition onto the target.

Figure 3(c) shows the fibres collected in the presence of enclosed-air-shield. Electrospinning with enclosed-air-shield improved the thickness of aligned nanofibres film to $4 \mu\text{m}$ and in 4 h, but the alignment was found to be poorer than that of obtained with top-air-shield as well as without shield setup. This result indicated that air flow exclusively towards the deposition area was influencing the alignment significantly. The installation of air-hood within the enclosed-air-shield as shown in Figure 1(d) allows collection of aligned nanofibres onto FTOs without much air

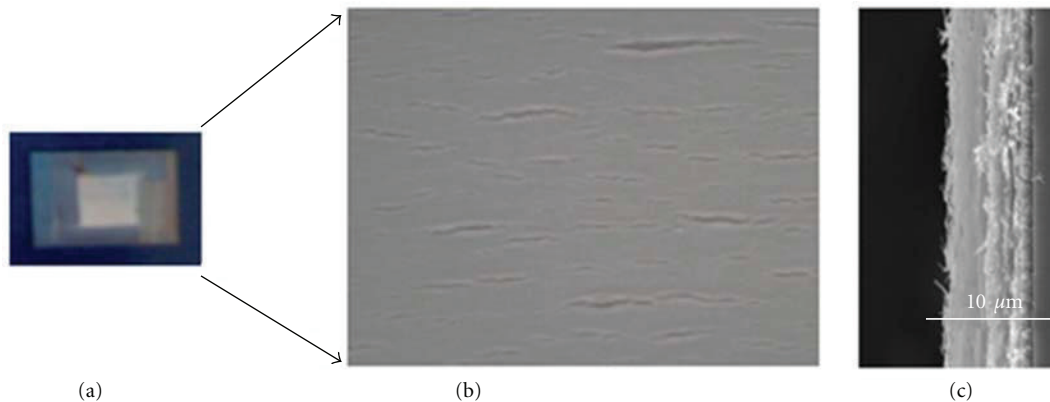


FIGURE 4: Sintered-aligned TiO_2 ceramic nanofibres. (a) Photo image, (b) optical microscope image (50x), and (c) SEM cross-sectional view of TiO_2 ceramic nanofibres.

disturbance. This configuration yielded two benefits: $4\ \mu\text{m}$ thick nanofibres were produced in 4 h, and better alignment.

A higher degree of fibres alignment was achieved by air-hood as shown in the SEM micrographs (Figure 3(d)). SEM Figure 3(d) shows that more than 80% were aligned to within $15\text{--}20^\circ$ of the average orientation. This could be attributed to the charges that each nanofibre acquires during the electrospinning. The distribution of the fibres across the gap became more stable. The enclosed air shield with air-hood produced the aligned TiO_2 nanofibres of $4\ \mu\text{m}$ thickness in 4 h. Earlier our group reported that time period of 8 h was required to obtain $4\ \mu\text{m}$ thick ZnO random nanofibres on FTO by simple electrospinning [22]. The shield not only reduced the collection time for obtaining same film thickness, but also allowed for well alignment of TiO_2 fibres on FTO substrates. The $4\ \mu\text{m}$ thick sintered TiO_2 nanofibres under microscope showed that there was no peeling-off problem upon sintering even after the thickness was increased higher, but few cracks along the fiber alignment direction (Figures 4(a) and 4(b)). It was also realized that the alignment of TiO_2 nanofibres at 750 rpm onto FTO itself increased the firmness to the fibres and adhesiveness to FTO. This was confirmed upon comparing the same thick but random TiO_2 nanofibres prepared on FTO without disc rotation. The fibers were found to be flaked off the FTO substrate upon annealing at 500°C . Investigation under SEM revealed that the alignment of the TiO_2 nanofibres was retained even at higher thickness after sintering at 500°C , indicating that the relaxation of residual stresses could be evenly distributed upon aligning the fibers.

Poor thickness of nanofiberous film is also connected to the lower flow rate of the precursor solution in electrospinning. Flow rate can be scaled up by increasing the needle diameter; however, it leads to large diameter fibres. Researchers have explored the possibility of both using multiple needles [23] and creating multiple holes in the single needle [24] in electrospinning. In this work, double-needle setup was fabricated for the collection of aligned TiO_2 nanofibres (Figure 5). In double-needle electrospinning, the distance between two needles is critical in producing the

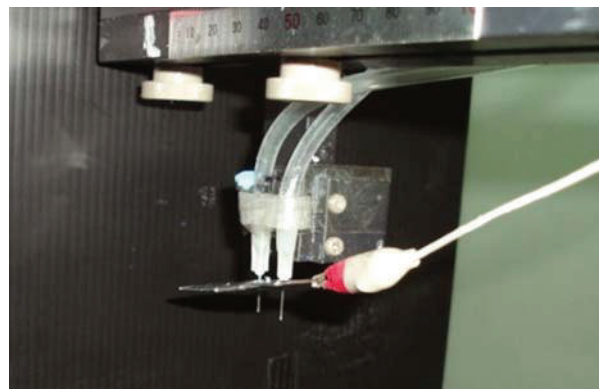


FIGURE 5: Photo image of double-needle arrangement for electrospinning.

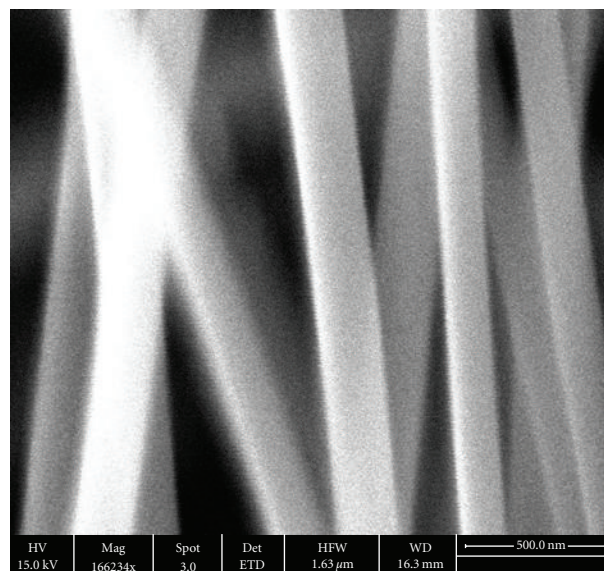


FIGURE 6: SEM image of aligned ceramic TiO_2 nanofibres using double-needle electrospinning.

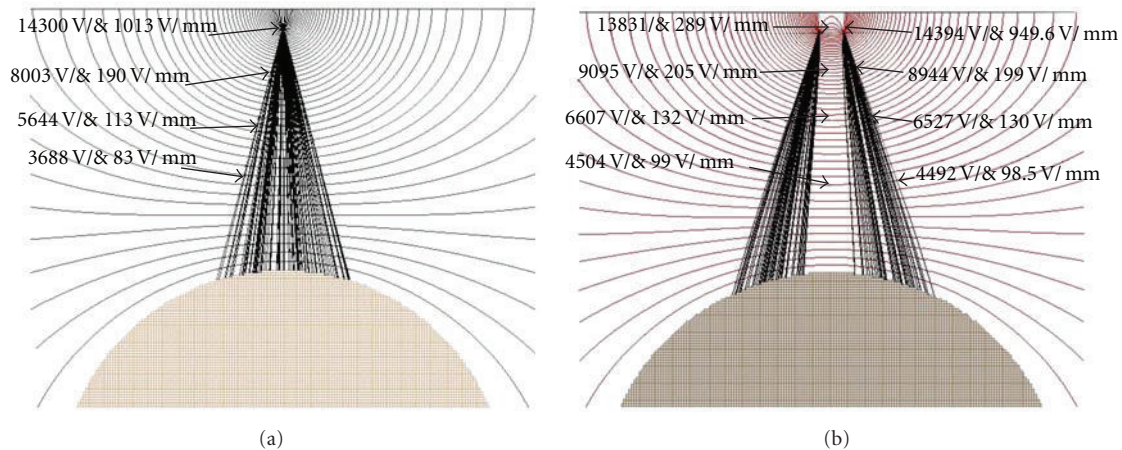


FIGURE 7: Theoretical prediction of flow of stream calculated based on 15 kV and the distance of 10 cm between needle tip and disc collector for (a) single-needle system and (b) double-needle system.

uniform nanofibres. In our study, the distance between the needles was optimized to 1 cm such that the repelling force between jets from two needles could be minimal. The same electrospinning condition was adopted for double-needle setup. The study using double needle with enclosed air-shield and air-hood yielded $6\ \mu\text{m}$ thick and aligned TiO_2 nanofibres in 4 h. TiO_2 nanofibres obtained using double-needle-based electrospinning were quite uniform in diameter (Figure 6), but was found to be smaller than that of fibres produced using a single-needle-based electrospinning. The diameter of the sintered fibres from the double needle was about $70 \pm 12\ \text{nm}$, whereas the sintered fibres obtained using the single needle possessed $98 \pm 20\ \text{nm}$. The difference in diameter could be due to following effects: the repulsive force from the two charged jet might involve in pulling of the nanofibres and secondly, stronger electric field leads to greater stretching of the jet and resulting in thin fibres.

Theoretical studies were carried out to correlate the difference in fibres diameter obtained from experiments. SIMION 8, an ion modeling package, was adopted to interpret the electrospinning jet based on the electric field distribution by estimating equipotential lines distribution around the electrodes as well as collector. For the same 15 kV potential and distance of 10 cm between the needle and disc collector, the simulation profiles on electrical distribution of the jet stream from both single-needle and double-needle system were obtained. Figure 7 shows the electric field distribution along the jet path for both single-needle and double-needle systems.

For the identical voltage, the electric field lines at the tip of the needle in double-needle arrangement was estimated to be lower compared to single-needle setup, indicating that the repulsive field plays a critical role in the double-needle system. At the area just below the needle tip, the electric field intensity for the double-needle setup was higher than that of single-needle setup. In the mid distance between the needle and collector, the electric field intensity was measured as $98.5\ \text{V/mm}$ for double needle, and $83\ \text{V/mm}$ for a single needle. The intensity of the electric field (V/m) at the various

position of the flow stream was measured to be stronger in double-needle system, suggesting that overstretching of the nanofibres were possible in double needle before deposition. Thus, the simulation study conveyed that the repulsive force of the charged fibers and the stronger electric field distribution along the flow of stream should play an influential role in reducing the fibers diameter.

4. Conclusions

Highly aligned ceramic TiO_2 nanofibres of diameter $98\ \text{nm}$ on FTOs were directly prepared using rotating disc-based electrospinning. With the ease of design, control over deposition, and the potential for continuous electrospinning, this study demonstrated the substantial improvement in the alignment (over 80%) of nanofiber by introducing an enclosed-air-shield and air-hood. Aligned nanofiberous film with the thickness adjustable from $100\ \text{nm}$ upto $6\ \mu\text{m}$ was demonstrated. We believe that the ability to prepare aligned and controlled thickness of nanofibres directly on the conductive substrates opens up potential opportunities in the domain of energy and electronics. There are still challenges that must be addressed in our approach: to reach above 80% alignment, thickness above $10\ \mu\text{m}$ in shorter time ($<4\ \text{h}$), and better understanding of the physics underlying alignment.

Acknowledgments

Authors acknowledge Singapore NRF-Technion Grant (WBS no: R-398-001-065-592) and Singapore NRF-NTU CRP Grant for the funding support.

References

- [1] M. Law, L. E. Greene, J. C. Johnson, R. Saykally, and P. Yang, "Nanowire dye-sensitized solar cells," *Nature Materials*, vol. 4, no. 6, pp. 455–459, 2005.
- [2] S. I. Na, S. S. Kim, W. K. Hong et al., "Fabrication of TiO_2 nanotubes by using electrodeposited ZnO nanorod template

- and their application to hybrid solar cells," *Electrochimica Acta*, vol. 53, no. 5, pp. 2560–2566, 2008.
- [3] T. Krishnamoorthy, V. Thavasi, G. M. Subodh, and S. Ramakrishna, "A first report on the fabrication of vertically aligned anatase TiO₂ nanowires by electrospinning: preferred architecture for nanostructured solar cells," *Energy & Environmental Science*, vol. 4, no. 8, pp. 2807–2812, 2011.
- [4] H. S. Shim, S. I. Na, S. H. Nam et al., "Efficient photovoltaic device fashioned of highly aligned multilayers of electrospun TiO₂ nanowire array with conjugated polymer," *Applied Physics Letters*, vol. 92, no. 18, Article ID 183107, 2008.
- [5] S. H. Choi, G. Ankonina, D. Y. Youn et al., "Hollow ZnO nanofibers fabricated using electrospun polymer templates and their electronic transport properties," *ACS Nano*, vol. 3, no. 9, pp. 2623–2631, 2009.
- [6] Y. Liu, J. Dong, and M. Liu, "Wll-aligned "nano-box-beams" of SnO₂," *Advanced Materials*, vol. 16, no. 4, pp. 353–356, 2004.
- [7] S. S. Kim, J. Jo, C. Chun, J. C. Hong, and D. Y. Kim, "Hybrid solar cells with ordered TiO₂ nanostructures and MEH-PPV," *Journal of Photochemistry and Photobiology A*, vol. 188, no. 2-3, pp. 364–370, 2007.
- [8] K. O. Hill and G. Meltz, "Fiber Bragg grating technology fundamentals and overview," *Journal of Lightwave Technology*, vol. 15, no. 8, pp. 1263–1276, 1997.
- [9] M. Lončar, T. Doll, J. Vučković, and A. Scherer, "Design and fabrication of silicon photonic crystal optical waveguides," *Journal of Lightwave Technology*, vol. 18, no. 10, pp. 1402–1411, 2000.
- [10] S. M. Yang and G. A. Ozin, "Opal chips: vectorial growth of colloidal crystal patterns inside silicon wafers," *Chemical Communications*, no. 24, pp. 2507–2508, 2000.
- [11] P. Katta, M. Alessandro, R. D. Ramsier, and G. G. Chase, "Continuous electrospinning of aligned polymer nanofibers onto a wire drum collector," *Nano Letters*, vol. 4, no. 11, pp. 2215–2218, 2004.
- [12] S. A. Theron, A. L. Yarin, E. Zussman, and E. Kroll, "Multiple jets in electrospinning: experiment and modeling," *Polymer*, vol. 46, no. 9, pp. 2889–2899, 2005.
- [13] A. L. Yarin and E. Zussman, "Upward needleless electrospinning of multiple nanofibers," *Polymer*, vol. 45, no. 9, pp. 2977–2980, 2004.
- [14] V. Thavasi, G. Singh, and S. Ramakrishna, "Electrospun nanofibers in energy and environmental applications," *Energy & Environmental Science*, vol. 1, no. 2, pp. 205–221, 2008.
- [15] J. A. Matthews, G. E. Wnek, D. G. Simpson, and G. L. Bowlin, "Electrospinning of collagen nanofibers," *Biomacromolecules*, vol. 3, no. 2, pp. 232–238, 2002.
- [16] D. Li and Y. Xia, "Direct fabrication of composite and ceramic hollow nanofibers by electrospinning," *Nano Letters*, vol. 4, no. 5, pp. 933–938, 2004.
- [17] K. Tennakone, G. R. R. A. Kumara, and K. G. U. Wijayantha, "The suppression of the recombination of photogenerated carriers in a dye-sensitized nano-porous solid-state photovoltaic cell," *Semiconductor Science and Technology*, vol. 11, no. 11, pp. 1737–1739, 1996.
- [18] B. O'Regan and D. T. Schwartz, "Large enhancement in photocurrent efficiency caused by UV illumination of the dye-sensitized heterojunction TiO₂/RuLL'NCS/CuSCN: initiation and potential mechanisms," *Chemistry of Materials*, vol. 10, no. 6, pp. 1501–1509, 1998.
- [19] U. Bach, D. Lupo, P. Comte et al., "Solid-state dye-sensitized mesoporous TiO₂ solar cells with high photon-to-electron conversion efficiencies," *Nature*, vol. 395, no. 6702, pp. 583–585, 1998.
- [20] J. Krüger, R. Plass, M. Grätzel, P. J. Cameron, and L. M. Peter, "Charge transport and back reaction in solid-state dye-sensitized solar cells: a study using intensity-modulated photovoltage and photocurrent spectroscopy," *Journal of Physical Chemistry B*, vol. 107, no. 31, pp. 7536–7539, 2003.
- [21] H. S. Shim, S. I. Na, S. H. Nam et al., "Efficient photovoltaic device fashioned of highly aligned multilayers of electrospun TiO₂ nanowire array with conjugated polymer," *Applied Physics Letters*, vol. 92, no. 18, Article ID 183107, 2008.
- [22] W. Zhang, R. Zhu, X. Liu, B. Liu, and S. Ramakrishna, "Facile construction of nanofibrous ZnO photoelectrode for dye-sensitized solar cell applications," *Applied Physics Letters*, vol. 95, no. 4, Article ID 043304, 2009.
- [23] F. L. Zhou, R. H. Gong, and I. Porat, "Mass production of nanofibre assemblies: by electrostatic spinning," *Polymer International*, vol. 58, no. 4, pp. 331–342, 2009.
- [24] F. L. Zhou, R. H. Gong, and I. Porat, "Three-jet electrospinning using a flat spinneret," *Journal of Materials Science*, vol. 44, no. 20, pp. 5501–5508, 2009.



Hindawi

Submit your manuscripts at
<http://www.hindawi.com>

